Title	Computation of transcritical steady flow over a curved bed with lateral contraction
Author(s)	Cheng, Nian-Sheng; Law, Adrian Wing-Keung; Lo, Edmond Yat-Man
Citation	Cheng N. S., Law, A. W. K. and Lo, E. Y. M. (2003). Transcritical flow over a moderately curved bed with lateral contraction. Journal of Hydraulic Research, 41(6), 631-637.
Date	2003
URL	http://hdl.handle.net/10220/7675
Rights	© 2003 IAHR. This is the author created version of a work that has been peer reviewed and accepted for publication by Journal of hydraulic research, International Association for Hydro-Environment Engineering and Research. It incorporates referee's comments but changes resulting from the publishing process, such as copyediting, structural formatting, may not be reflected in this document. The published version is available at: [DOI: http://dx.doi.org/10.1080/00221680309506895].

COMPUTATION OF TRANSCRITICAL FLOW OVER A CURVED BED WITH LATERAL CONTRACTION

Nian-Sheng Cheng, Adrian W. K. Law, and Edmond Y. M. Lo

School of Civil and Structural Engineering, Nanyang Technological University
Nanyang Avenue, Singapore, 639798.

Abstract: A one-dimensional equation is derived to compute the water surface profile for transcritical flows over a moderately curved bed combined with lateral contraction. The effect of the flow curvature is included as a pressure correction in the momentum equation. The computed flow profiles compare well with the experimental data.

Key words: Transcritical flow; curved bed; lateral contraction; water surface profile.

Introduction

The classical St. Venant equations are widely used in solving long wave problems encountered in hydraulic engineering. Numerical computations in the literature have shown that the equations are adequate in simulating the free-surface flow over lightly curved beds. As the equations are derived with an assumption of the hydrostatic pressure distribution, however, they have been found insufficient when applied to some moderately to highly curved flows such as those caused by hydraulic structures, bed-form and contractions.

One of the improvements on the St. Venant equations is due to Dressler (1978), who derived a set of shallow-water equations for irrotational flows using a curvilinear

coordinate system based on the curved bed profile. Sivakumaran and Yevjevich (1987) have shown that the Dressler's equations work well for the flow over a highly curved spillway. The predicted free-surface profiles and bed pressures are in better agreement with the measurements than those computed using the St. Venant equations. However, the Dressler's theory can only be applied within a subcritical or supercritical regime, and appears to falter in the case of transcritical flows when the regime transits from subcritical to supercritical (Sivakumaran, et al. 1983; Fenton, 1996).

Alternatively, Steffler and Jin (1993) obtained a horizontal momentum equation by averaging vertically the two-dimensional Reynolds equations. As special velocity and pressure corrections are included in the horizontal momentum equation, Steffler and Jin also proposed additional equations to specify the related correction parameters. This finally leads to a system of five equations that are much more complicated than the St. Venant equations. Khan and Steffler (1995, 1996) showed that such a system can be applied to the case of transcritical flows over curved beds. Fenton (1996) incorporated the centrifugal effect on the pressure distribution into the long wave equation using the control volume method. Numerical simulations show his equation works for the transition from subcritical to supercritical flow. The Fenton's approach was also employed by Law (1997) to investigate a steady flow over an obstacle with geometric changes in both the sidewall and bottom boundaries. The preliminary computation conducted by Law shows that the curvature effect from the surface elevation is minimal compared to the bottom elevation.

The objective of this paper is to investigate transcritical flows subjected to a moderately curved bed together with a combined lateral contraction. This combination of sill and contraction is a rather common feature for many hydraulic control structures. Most of the previous studies focus only on the effect of the bottom elevation changes. In comparison, the effect of the lateral contraction with the simultaneous bottom changes has not been well studied. A new one-dimensional momentum equation is derived with special considerations on only the pressure correction for this case. The water-surface profiles computed with different kinds of pressure correction are compared with the

experimental data. The agreement is satisfactory demonstrating the validity of the approach towards the one-dimensional simulation of transcritical flows.

Derivation of Governing Equation

Consider a steady open-channel flow over an obstacle where the cross-section is rectangular but subject to continuous geometric changes in both the bottom and side boundaries. A one-dimensional governing equation can be obtained by applying the momentum principle to a control volume, as shown in Fig. 1, which is located at a cross section and extends a distance *dx* in the horizontal direction.

The change of the momentum of the fluid mass through the control volume is

$$M = \frac{d}{dx}\left(\frac{Q^2}{BH}\right) \tag{1}$$

where Q = flow rate, B = width of the channel and H = water depth. The forces acting on the fluid mass consist of the pressure difference on the cross section P_1, the horizontal component of the normal pressure exerted by the bottom and the sidewall P_2, and the friction drag F. If the cross-sectional pressure is assumed to be distributed linearly, P_1 and P_2 can be related to the bottom pressure P_b, respectively, as follows:

$$P_1 = -\frac{d}{dx}\left(\frac{P_b BH}{2\rho}\right) \tag{2}$$

$$P_2 = \frac{P_b H}{2\rho}\frac{dB}{dx} - \frac{P_b B}{\rho}\frac{dh}{dx} \tag{3}$$

where h = bottom elevation. The friction drag can be expressed in terms of the friction slope S_f in the form:

$$F = -gBHS_f \tag{4}$$

where g = gravitational acceleration.

Summation of all the forces acting on the fluid mass, according to the momentum principle, is equal to the momentum change, yielding

$$\frac{d}{dx}\left(\frac{Q^2}{BH}\right)+\frac{d}{dx}\left(\frac{P_b BH}{2\rho}\right)-\frac{P_b H}{2\rho}\frac{dB}{dx}+\frac{P_b B}{\rho}\frac{dh}{dx}+gBHS_f=0 \tag{5}$$

Bottom Pressure

For moderately curved flows, the pressure is dominated by the hydrostatic component. However, there also exists a hydrodynamic pressure component due to the flow curvature, which can be viewed as a correction to the overall fluid pressure. The bottom pressure P_b included in (5) can thus be written as:

$$P_b = P_{b1} + P_{b2} \tag{6}$$

where $P_{b1} = \rho g H$, and P_{b2} = component due to curved flow. If P_{b2} is equal to zero, (5) reduces to the St. Venant momentum equations. Fenton (1996) assumed that the effect of the curvature could be incorporated into the hydrodynamic correction pressure in the form of

$$p = \int\left[-\rho g - \frac{\rho Q^2}{B^2 H^2}\left(w_0 \frac{h''}{1+h'^2} + w_1 \frac{H''}{1+H'^2}\right)\right]dz \tag{7}$$

where p = pressure at the elevation z; w_o, w_1 = constants; $(\,)' = d(\,)/dx$; and $(\,)'' = d^2(\,)/dx^2$. Integrating (7) from $z = h$ to $z = h + H$, one can get

$$P_b = \rho g H + \frac{\rho Q^2}{B^2 H}\left(w_0 \frac{h''}{1+h'^2} + w_1 \frac{H''}{1+H'^2}\right) \tag{8}$$

Note that in (8) the bottom portion for the expression of the flow curvature was simplified to yield a simpler set of governing equations for computation purposes. Substitution of (8) into (5) leads to a governing equation which was used in Law (1997). For two sets of values for the constants w_o and w_1, Law found that the numerical results of the water surface profile deviate obviously from his measurements even before the transition point.

Steffler and Jin (1993) found that for curved flows, the correction to the bed curvature can be related to the effects of the centrifugal force, the vertical component of the shear stress, and contributions from the non-uniform velocity distribution. If only the effect of the centrifugal force is considered, the relationship given by Steffler and Jin can be reduced for steady flows to the form (Khan and Steffler, 1995):

$$P_{b2} = \frac{d}{dx}\left(\frac{dz_c}{dx}\frac{\rho Q^2}{B^2 H}\right) \tag{9}$$

where z_c = characteristic elevation used to describe the effect of the centrifugal force caused by the flow curvature. This elevation can be taken at the mid-depth, i.e.

$$z_c = h + \frac{H}{2} \tag{10}$$

Substitution of (9) and (10) into (6), one gets

$$P_b = \rho g H + \rho \frac{d}{dx}\left[\frac{Q^2}{B^2 H}(h' + \frac{H'}{2})\right] \tag{11}$$

Compared to (8), (11) does not include any undetermined coefficients. By substituting (11) into (5), a governing equation can be obtained in the form of a third-order ordinary differential equation for the water surface elevation:

$$\eta''' - \left(\frac{2H'}{H} + \frac{4B'}{B}\right)\eta'' + \left(\frac{4gB^2H}{Q^2} + \frac{H'^2 - h'H' - 3h'^2 - 4}{H^2} + \frac{2B'H' - 2B'h'}{BH} + \frac{6B'^2 - 2BB''}{B^2}\right)\eta' + \frac{4gS_f B^2 H}{Q^2} + \frac{6B'^2 h' - 4BB'h'' - 2BB''h'}{B^2} - \frac{4B' + 6B'h'^2}{BH} + \frac{4h'h''H + 4h' + 3h'^3 + h'''H^2}{H^2} = 0 \quad (12)$$

where $\eta' = h + H$ = water surface elevation and $(\,)''' = d^3(\,)/dx^3$.

In fact, the bottom pressure can be theoretically related to the flow parameters like flow rate and water depth. This can be done by integrating the vertical momentum equation along the water depth. If the diffusion term in the vertical momentum equation can be ignored, the integration yields

$$P_b = \rho g H + \rho \frac{d}{dx}\left(\int_h^{h+H} uw\,dz\right) \quad (13)$$

where u = horizontal velocity; and w = vertical velocity. Following Steffler and Jin's (1993) study, the horizontal velocity distribution is expressed to be

$$u = U + (u_s - U)\left(2\frac{z-h}{H} - 1\right) \quad (14)$$

and the vertical velocity distribution reads

$$w = w_b\left(1 - \frac{z-h}{H}\right) + w_s\frac{z-h}{H} + 4w_c\frac{z-h}{H}\left(1 - \frac{z-h}{H}\right) \quad (15)$$

where U = depth-averaged horizontal velocity; u_s = horizontal velocity at the surface elevation; w_b = vertical velocity at the bottom elevation; w_s = vertical velocity at the

surface elevation; and w_c = vertical velocity at the mid-depth. Substituting (14) and (15) into (13) yields

$$P_b = \rho g H + \rho \frac{d}{dx}\left[\frac{U(w_b + w_s)}{2} + \frac{(u_s - U)(w_s - w_b)}{6} + \frac{2Uw_c}{3}\right] \tag{16}$$

Furthermore, if the vertical velocity is approximately uniformly distributed along the water depth, i.e., $w_b \approx w_s$ and $w_c \approx 0$, (16) changes to

$$P_b = \rho g H + \rho \frac{d(Uw_s)}{dx} \tag{17}$$

With reference to Khan and Steffler (1995), w_s is approximated in the form

$$w_s = U\frac{d(h+H)}{dx} \tag{18}$$

Substitution of (18) into (17) gives

$$P_b = \rho g H + \rho \frac{d}{dx}\left(\frac{Q^2}{B^2 H}\eta'\right) \tag{19}$$

Obviously, (19) is the same as (11) if the characteristic elevation z_c in (9) is taken at the water surface instead of the mid-depth. The physical meaning related to (19) can be further explained in the following. As implied by Steffler and Jin (1993), the curvature of the mid-depth elevation in the open-channel flow can be used to represent the effect of the curved flow on the water surface profile. However, it may not be true when the water surface elevation changes in a way that opposes the bed slope. For example, the elevation profile at the mid-depth upstream of a bed hump exhibits an obvious curvature while the water surface profile does not for the same horizontal location. Under such conditions, some errors may be involved in the computation of the water surface profile if the curvature at the mid-depth is still used to represent the effect of the curved flow on the

water surface profile. Alternatively, it is more reasonable to take the characteristic elevation of the flow at the water surface, as shown in (19).

By substituting (19) into (5), another governing equation can thus be obtained as follows**:**

$$\eta''' + \left(\frac{h'}{H} - \frac{2H'}{H} - \frac{4B'}{B}\right)\eta'' + \left(\frac{2gB^2H}{Q^2} + \frac{h''H + H'^2 - 2h'H' - 2}{H^2} + \frac{2B'H' - 4B'h'}{BH} + \frac{6B'^2 - 2BB''}{B^2}\right)\eta' + \frac{2gS_fB^2H}{Q^2} + \frac{2Bh' - 2B'H}{BH^2} = 0 \tag{20}$$

Furthermore, it is possible to ignore the longitudinal variation of $\rho Q/(B^2H)$ in (19) when the water surface is significantly curved. Therefore, an alternative to (19) thus reads

$$P_b = \rho gH + \frac{\rho Q^2}{B^2H}\eta'' \tag{21}$$

Substitution of (21) into (5) yields

$$\eta''' + \left(\frac{2h'}{H} - \frac{2B'}{B}\right)\eta'' + \left(\frac{2gB^2H}{Q^2} - \frac{2}{H^2}\right)\eta' + \frac{2gS_fB^2H}{Q^2} + \frac{2Bh' - 2B'H}{BH^2} = 0 \tag{22}$$

Eq. (22) is much simpler than (12) and (20).

In the following, (12), (20) and (22) are solved using the fourth-order Runge-Kutta numerical scheme. The friction slope S_f included in these equations is related to the Manning roughness coefficient n in the form:

$$S_f = \left(\frac{Qn}{BH}\right)^2\left(\frac{2H + B}{BH}\right)^{4/3} \tag{23}$$

where n = coefficient of roughness of the boundary. Numerical solutions to water surface profiles and bed pressure distributions are investigated for the feasibility of the derived governing equations in simulating transcritical flows over a bottom sill with or without lateral contraction.

Experiments

To verify the approach proposed in the present study, the computation results are compared to experimental data documented, respectively, in Sivakumaran et al. (1983) and Law (1985). Sivakumaran et al. conducted a series of experiments for open-channel flows over a bed sill without lateral contraction. On the other hand, Law's study aimed to investigate the water surface profile due to transcritical flows passing through a combined sill and lateral contraction.

Flow over a Pure Sill

In Sivakumaran et al. (1983)'s experiments, a symmetric bed profile was designed according to the normal distribution as follows:

$$h = 0.2\exp\left(-\frac{x^2}{0.1152}\right) \tag{24}$$

where h and x are measured in m. They performed the experiments in a flume that is 9.2 m long and 0.3 m wide. Along the centerline of the curved bed, both the water surface profile and the bottom pressure were measured at 0.05 m horizontal intervals for steady flows.

Flow over a Sill Combined with Lateral Contraction

Law (1985) conducted his experiments in a 16 m long recirculating flume. At the middle section of the flume, a curvilinear obstacle made of Plexiglass was installed to induce the

geometrical changes along the sidewall and the flume bottom. The resulting bed surface profile and width of the open-channel are described, respectively, in the form:

$$h = h_o\left[0.05 + \cos^2\left(\frac{x-S}{3h_o}\right)^2\right] \qquad \text{for } |x| \le 1.5\pi h_o \tag{25}$$

$$B = B_o\left[1 - 0.4\cos^2\left(\frac{x}{3h_o}\right)\right] \qquad \text{for } |x-S| \le 1.5\pi h_o \tag{26}$$

where h_o = 0.06 *m*; S = 0.2 *m*; and B_o = uncontracted channel width = 0.157 *m*. The sidewall contraction protrudes from one side of the channel, as shown in Fig. 2. The maximum lateral contraction in the channel locates at x = 0 and the highest bed elevation is 0.1 m downstream of the maximum lateral contraction. The design of the obstacle incorporates two objectives: (1) the minimum radius of curvature of the bottom sill is much larger than the flow depth in the experiments such that the approach of modeling the pressure term as a hydrostatic component with a hydrodynamic correction remains valid, and (2) the range of the critical locations that correspond to the range of discharge in the experiments would be around the middle of the sill crest and the minimum contraction. This way both the sill and the contraction will play a significant role in controlling the water flows.

The discharge in the recirculating flume was recorded using an orifice meter with an estimated accuracy of within 2%. The water surface profile was taken using point gauges at the middle of the cross-section. The accuracy of the point gauge measurements was within 0.3 mm. The measurement error of the surface elevation was thus typically less than 0.5% of the total flow depth. Due to the contraction and the fact the obstacle is not symmetrical, there is a slight tilting of the water surface in the lateral direction. The tilting was more prominent in the supercritical region. However, at any particular location near the critical region the amount of tilting was observed to be less than 5% of the water depth readings taken at the middle of the cross-section.

Computation and Comparison

For each case studied in this paper, only the flow rate is given as the upstream boundary condition. This is because for a subcritical flow, it is necessary to impose two boundary conditions, respectively, at the upstream and downstream ends; while two conditions are needed for a subcritical flow only at the upstream end (for example, Meselhe et al., 1997). Therefore, only one condition is required at the upstream boundary when the flow changes from subcritical regime to supercritical regime.

In implementing the Runge-Kutta numerical scheme in the computation, the water surface elevation at the upstream boundary is considered unknown until the stable solution to the water surface profile is achieved, i.e., a shooting method is used. In addition, the upstream boundary is taken, for example, at x = -2.0 m, which is far from the rapidly-varied section in the channel. This is to ensure that the second and third derivatives of the water surface elevation can be set to zero at the upstream boundary corresponding to negligible curvature effects. The first derivative of the water surface elevation at the upstream boundary is then evaluated using the governing equations. It should be noted that the computation requires an accuracy control with low tolerance. Otherwise, the iterative process may be subjected to parasitic solutions which were reported by both Fenton (1996) and Law (1997).

Fig. 3 shows comparison of the computed water surface profiles over the pure sill with the measured results reported by Sivakumaran et al. (1983) for Q = 0.0336 m^3/s. The water surface elevation immediately upstream of the sill computed using (12) is slightly lower than that using (22). However, the three profiles predicted are all quite close to the measured data. Given the predicted water surface profiles, the bed pressure can be computed, respectively, using (11), (19) or (21). The results obtained are plotted in Fig. 4, showing that the bed pressure distributions predicted using (11) and (19) are in good agreement with the experimental data while the prediction using (21) is higher in the downslope zone of the sill. The difference between the distributions predicted using (19) and (21) is found to be caused by the simplification introduced in deriving (21), i.e., the

neglect of the longitudinal variation of $\rho Q/(B^2H)$, though the simplification does not have significant influences on the prediction of the water surface profile, as shown in Fig. 3.

The numerical computations for flows over a sill combined with lateral contraction are conducted for the three experiments with flow rates of 0.00926 m^3/s, 0.00892 m^3/s and 0.00614 m^3/s. Fig. 5 shows the water surface profiles computed using the three governing equations. They are reasonably close to one another for all the three cases except for the transitional region around the control section. The critical control section at which the Froude number equals one is located at x = 0.13 m for Q = 0.00926 cm^3/s and 0.00892 cm^3/s, and x = 0.15 m for Q = 0.00614 m^3/s. The figure also shows that the flow profiles predicted using (20) and (22) are much closer to the measurements than those corresponding to (12). This suggests that the earlier consideration on the pressure correction, i.e. (19), is acceptable. It should be noted that there exist discontinuities of the derivatives of h at the ends of the sill profile and those of B at the ends of the sidewall contraction, which are described, respectively, in (25) and (26). These discontinuities were smoothed out in the computation by interpolating the values of the derivatives locally. Fig. 6 shows the corresponding bed pressure distributions predicted using (11), (19) and (21), respectively, for the three flow rates. The bed pressure obtained using (11) is significantly smaller around the transitional zone, while the computed results using (21) is higher but very close to that using (19).

The comparisons for the above two situations demonstrate that the equations, (20) and (22), derived in this paper are suitable for flows over curved beds, even with lateral contractions. However, the cases studied only concern the curved beds with the moderate curvature as defined in Sivakumaran et al. (1983), i.e. the relative curvature, $|kH| < 0.5$, where k = curvature of the bed and H = water depth. For example, in the case of the pure sill computed, the kH-values is found varying from – 0.39 to 0.42. In the case of the sill combined with the lateral contraction, the kH-values vary from – 0.28 to 0.29 for the largest flow rate, Q = 0.00926 m^3/s, and from – 0.23 to 0.24 for the smallest flow rate, Q = 0.00614 m^3/s. Therefore, further study is required to simulate flows over highly-curved beds.

CONCLUSIONS

The curvature of the water surface profile is included to correct the pressure term in the one-dimensional momentum equation for open channel flow. The governing equation, (20) and (22) , derived in this study can be used to predict the flow profile over a moderately-curved bottom sill with the presence of a combined lateral contraction. The predicted flow profiles are in good agreement with experiment results.

APPENDIX 1. REFERENCES

1. Dressler, R. F. (1978). "New nonlinear shallow flow equations with curvature." Journal of Hydraulic Research, IAHR, The Netherlands, 16(3), 205-222.
2. Fenton, J. D. (1996). "Channel flow over curved boundaries and a new hydraulic theory." Proc., 10th Congress of APD-IAHR, Langkawi, Malaysia. Vol. 2, 266-273.
3. Khan, A. A. and Steffler, P. M. (1995). "Discussion of 'Potential-flow solution to 2D transition from mild to steep slope' by J. S. Montes." Journal of Hydraulic Engineering, ASCE, 121(9), 680-682.
4. Law, A. W. K. (1985). "Single layer flow over an obstacle consisting of a contraction and sill." Hydraulic Engineering Laboratory Report No. UCB/HEL-85/06, Department of Civil Engineering, University of California at Berkeley.
5. Law, A. W. K. (1997). "Steady flow over an obstacle with contraction and sill." Proceedings of Theme A, Managing Water: Coping with Scarcity and Abundance, 27th IAHR Congress, San Francisco, pp.787-792.
6. Meselhe, E. A., Sotiropoulos, F., and Holly Jr., F. M. (1997). "Numerical simulation of transcritical flow in open channels." Journal of Hydraulic Engineering. ASCE, 123(9), 774-783.
7. Sivakumaran, N. S., Tingsanchali, T. and Hosking, R. J. (1983). "Steady shallow flow over curved beds." Journal of Fluid Mechanics, 128, 469-487.
8. Sivakumaran, N. S., and Yevjevich, V. (1987). "Experimental verification of the Dressler curved-flow equations." Journal of Hydraulic Research, IAHR, The Netherlands, 25(3), 373-391.

9. Steffler, P. M., and Jin, Y. -C. (1993). "Depth averaged and moment equations for moderately shallow free surface flow." Journal of Hydraulic Research, IAHR, The Netherlands, 31(1), 5-17.

APPENDIX 2. NOTATION

The following symbols are used in this paper:

B = width of the channel;
B_o = uncontracted width;
F = friction drag;
g = gravitational acceleration;
H = water depth;
h = bed elevation;
h_o = characteristic height at the highest bed elevation;
k = curvature of the bed surface;
n = Manning roughness coefficient;
p = pressure at the elevation z;
P_1 = pressure difference on the cross section;
P_2 = horizontal component of the normal pressure on the boundary;
P_b = bottom pressure;
P_{b1} = $\rho g H$;
P_{b2} = component of the bed pressure due to curved flow;
Q = flow rate;
S = distance between the maximum contraction and the highest bed elevation;
S_f = friction slop;
W_0 = constant;
W_1 = constant;
x = horizontal coordinate;
z = elevation;
z_c = characteristic elevation
η = $h + H$ = water surface elevation; and
ρ = density of fluid.

Supercript

$'$ = d/dx;
$''$ = d^2/dx^2; and
$'''$ = d^3/dx^3.

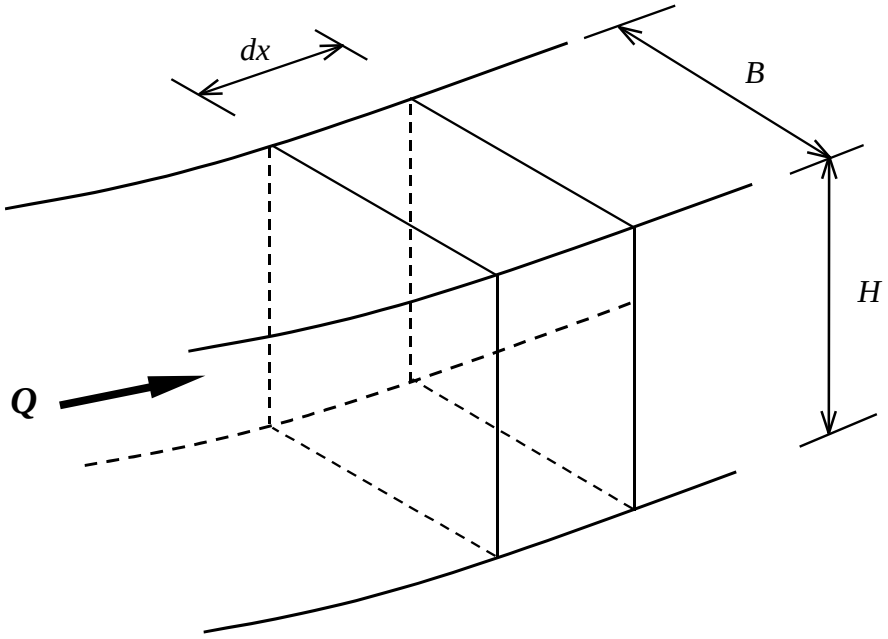

Fig. 1. Definition Sketch of Control Volume.

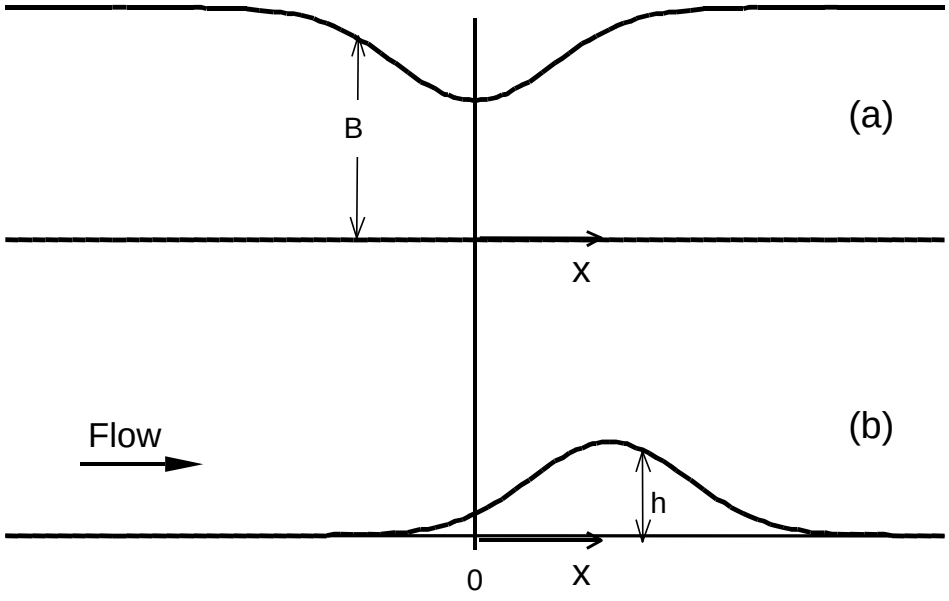

Fig. 2. Curved Bed and Sidewall Contraction:

(a) Plan view; (b) Elevation view.

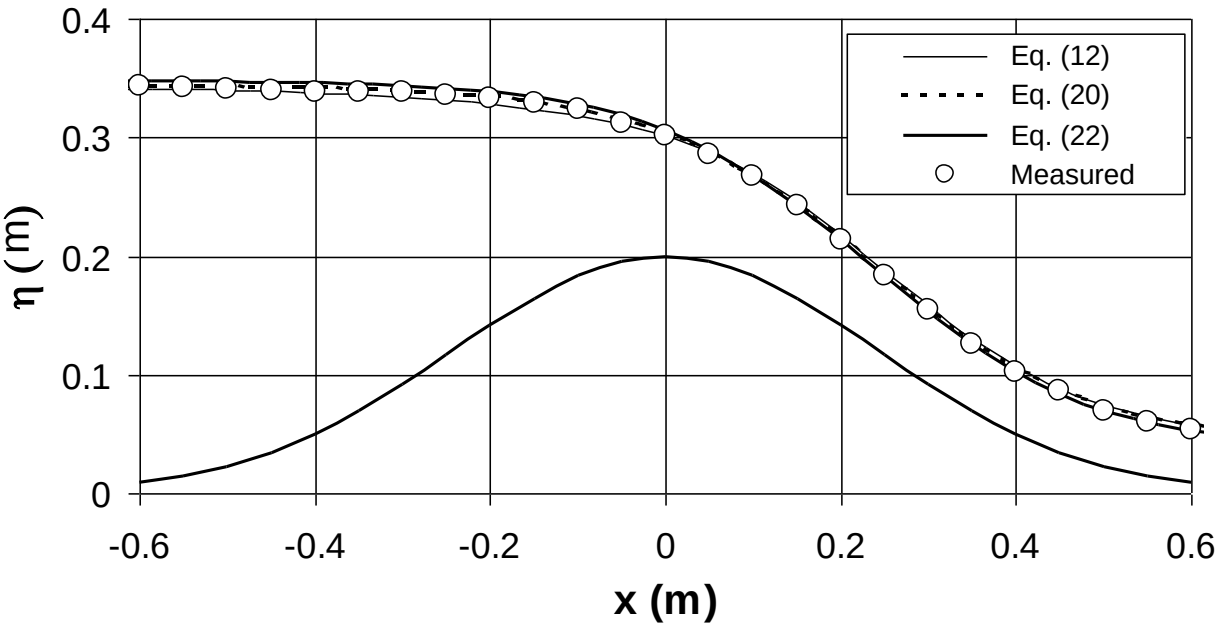

Fig. 3. Water Surface Profiles over a Pure Sill Compared with the Measurements by Sivakumaran et al. (1983).

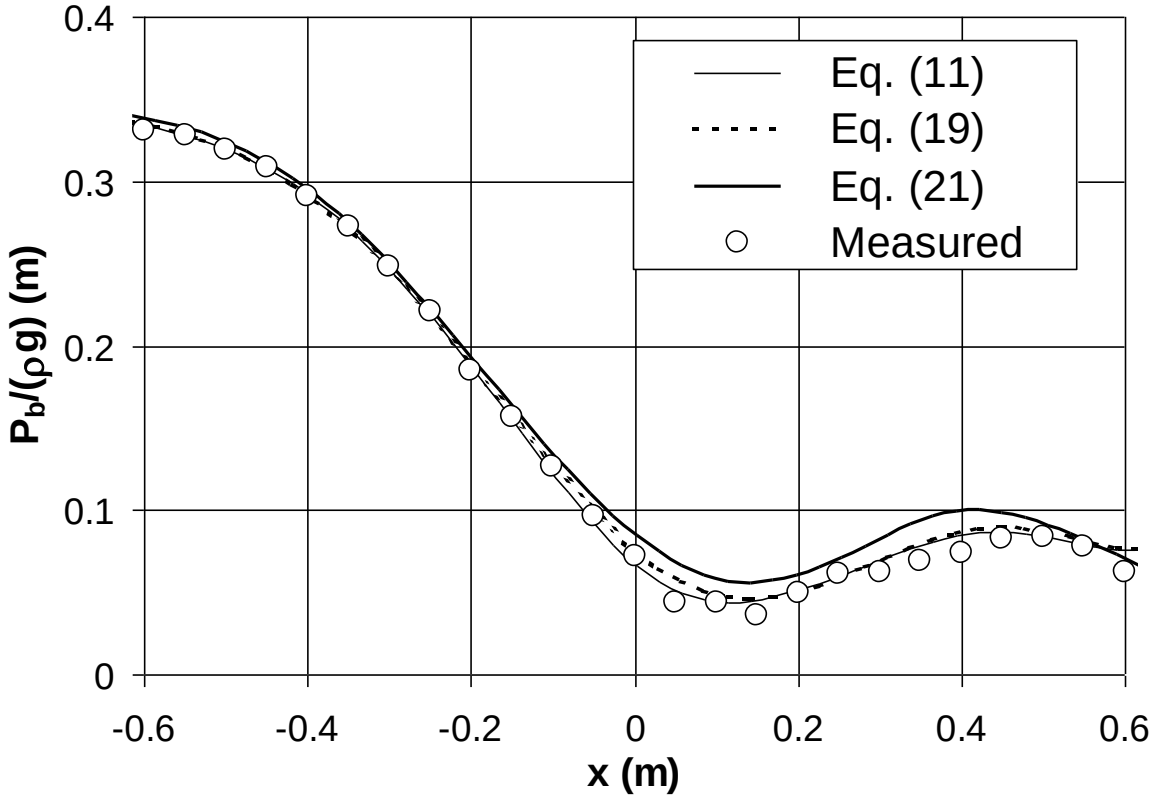

Fig. 4. Bed Pressure Distributions over a Pure Sill Compared with the Measurements Sivakumaran et al. (1983).

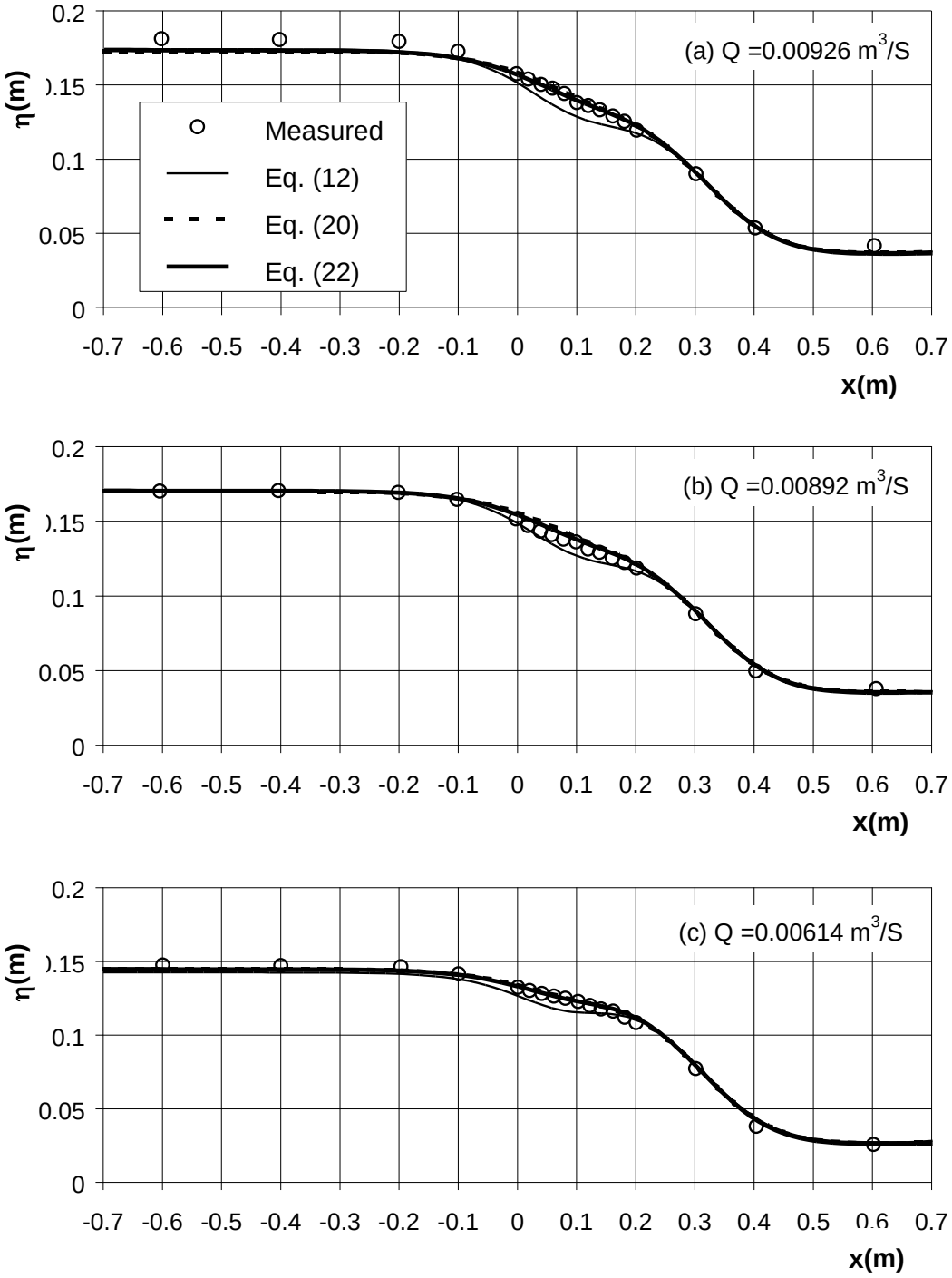

Fig. 5. Comparison with Experimental Data (Law, 1985) of Water Surface Profiles over a Sill Subjected to Lateral Contraction.

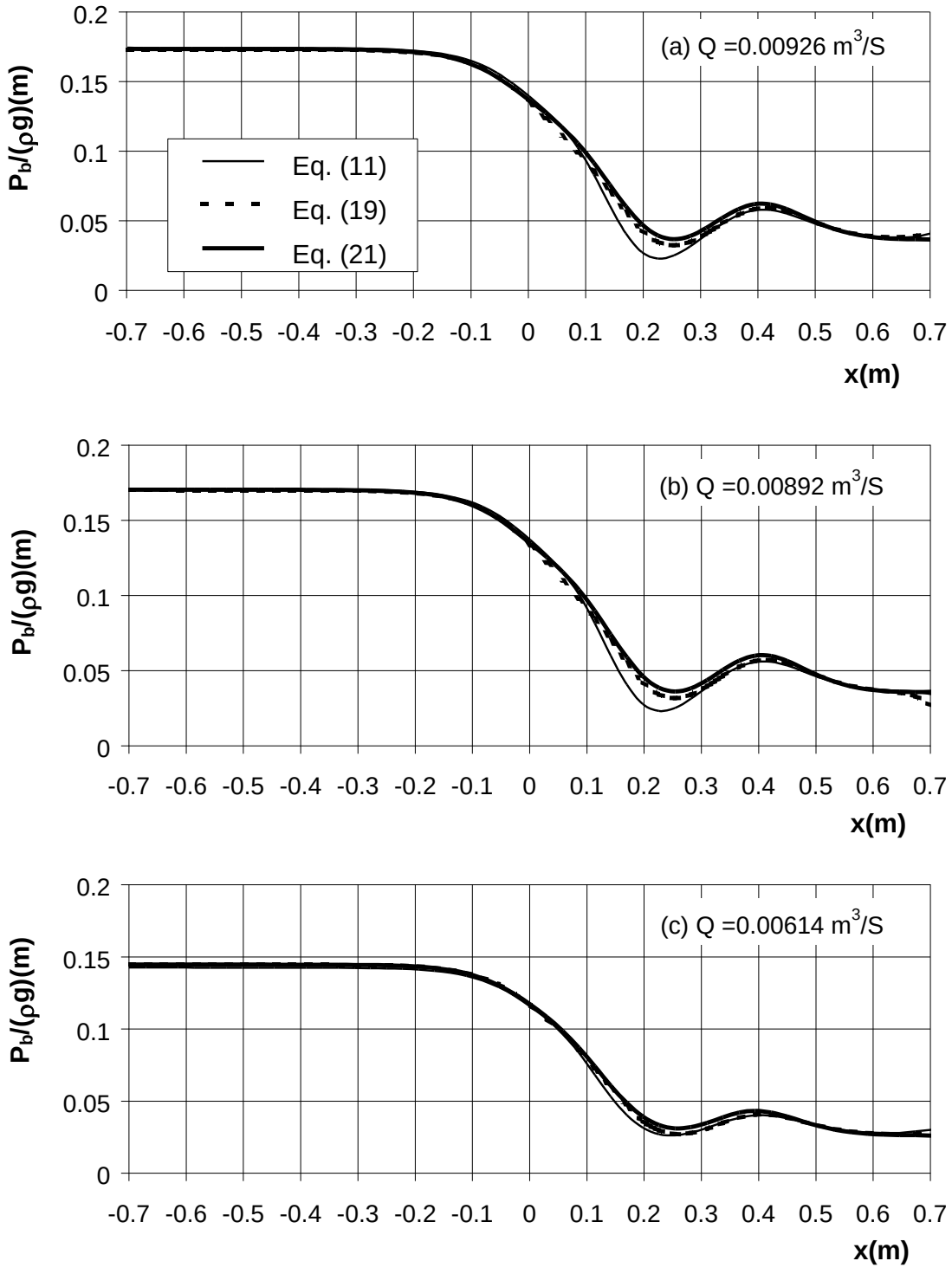

Fig. 6. Computed Bed Pressure Distributions over a Sill Subjected to Lateral Contraction.